

Supramolecular Chemistry

How to cite:

International Edition: doi.org/10.1002/anie.202102774

German Edition: doi.org/10.1002/ange.202102774

Metal Complex Lipids for Fluid–Fluid Phase Separation in Coassembled Phospholipid Membranes

Ryo Ohtani,* Yuka Anegawa, Hikaru Watanabe, Yutaro Tajima, Masanao Kinoshita,* Nobuaki Matsumori, Kenichi Kawano, Saeko Yanaka, Koichi Kato, Masaaki Nakamura, Masaaki Ohba, and Shinya Hayami*

Abstract: We demonstrate a fluid–fluid phase separation in 1,2-dimyristoyl-*sn*-glycero-3-phosphocholine (DMPC) membranes using a metal complex lipid of type [Mn(L1)] (**1**; HL1 = 1-(2-hydroxybenzamide)-2-(2-hydroxy-3-formyl-5-hexadecyloxybenzylideneamino)ethane). Small amount of **1** produces two separated domains in DMPC, whose phase transition temperatures of lipids (T_c) are both lower than that of the pristine DMPC. Variable temperature fluorescent microscopy for giant-unilamellar vesicles of DMPC/**1** hybrids demonstrates that visible phase separations remain in fluid phases up to 37°C, which is clearly over the T_c of DMPC. This provides a new dimension for the application of metal complex lipids toward controlling lipid distributions in fluid membranes.

Amphiphilic molecules form high-order structures via self-assemblies in solutions.^[1] Nature utilizes amphiphiles in constructing multicomponent coassembly systems in various fields.^[2] Coassembling is a ubiquitous strategy to improve functionalities. It has also been employed in material designs to achieve morphology control, tunable energy transport processes, high charge carrier mobility, and long phosphorescence with high stability.^[3] Recently, “phase separation” in such coassembled systems has been proposed as a key to

understand functionalities and formation mechanisms of coassemblies.^[4] Notably, cell membranes form fluids. However, “heterogeneous” coassembled platforms with fluid–fluid phase separation systems formed by thousands of lipids allow laterally separated domains to precisely manipulate biofunctions.^[2a,5,6] On the other hand, the chemical control of phase separation in fluid coassemblies of lipids is still difficult owing to the uncontrollable and high miscibility of lipid molecules.

Metal complex lipids are versatile materials. Their hydrophilic domains consist of metal complex moieties with catalytic, fluorescent, and transportation properties.^[1b,7] Such metal complex heads exhibit stronger electronic interaction with natural lipids than organic molecules; thus, they can be used to impact and modulate some properties of multilipid coassemblies such as miscibility and phase transition. Based on this, synthetic approaches for generating artificially separated “rigid” regions with regular structures by metal complex lipids in 1,2-dimyristoyl-*sn*-glycero-3-phosphocholine (DMPC) and cell membranes have been demonstrated.^[8] However, the development of artificial lipids those can produce stable “fluid” domains separated by other fluid regions in coassemblies remains largely unexplored.

Herein, we demonstrate the first example of a fluid–fluid phase separation in natural lipid membranes of DMPC by coassembling single-chain metal complex lipids of type [Mn(L1)] (**1**; HL1 = 1-(2-hydroxybenzamide)-2-(2-hydroxy-3-formyl-5-hexadecyloxybenzylideneamino)ethane). By the introduction of **1** to DMPC membranes, two fluid domains formed separately; the separation was maintained up to 37°C in the fluid membranes. We discovered that the intermolecular interaction of the metal complex cores with the aldehyde groups of **1** and phosphate groups in DMPC gave rise to phase separations.

Two amphiphilic ligands HL1 and 1-(2-hydroxybenzamide)-2-(2-hydroxy-5-hexadecyloxybenzylideneamino)ethane (HL2) were synthesized by a stepwise method (see the experimental section in supporting information). The metal complex lipids **1** and [Mn(L2)] (**2**) were synthesized by mixing the corresponding ligands with Mn(OAc)₂·4H₂O, which yielded their brown powders. Single crystals of **1**·3H₂O and **2**·2MeOH were obtained through their recrystallizations using suitable alcohols. **1**·3H₂O and **2**·2MeOH crystallized in triclinic *P*₁ and monoclinic *P*₂₁/*c*, respectively (Figure 1 and Table S1). X-ray structural analyses revealed structural differences in manganese complex cores of the metal complex lipids in which **1** incorporates **L1** with an aldehyde substituent, whereas, **2** consists of a similar ligand **L2** but without

[*] Prof. R. Ohtani, H. Watanabe, Y. Tajima, Dr. M. Kinoshita, Prof. N. Matsumori, Prof. M. Ohba
 Department of Chemistry, Faculty of Science, Kyushu University
 744 Motooka, Nishi-ku, Fukuoka 819-0395 (Japan)
 E-mail: ohtani@chem.kyushu-univ.jp
 kinoshi@chem.kyushu-univ.jp

Y. Anegawa, Prof. M. Nakamura, Prof. S. Hayami
 Department of Chemistry, Graduate School of Science
 Kumamoto University
 2-39-1 Kurokami, Chuo-ku, Kumamoto 860-8555 (Japan)
 E-mail: hayami@kumamoto-u.ac.jp

Dr. K. Kawano
 Institute for Chemical Research, Kyoto University
 Uji, Kyoto 611-0011 (Japan)

Dr. S. Yanaka, Prof. K. Kato
 Exploratory Research Center on Life and Living Systems (ExCELLS)
 and Institute for Molecular Science (IMS)
 National Institutes of Natural Sciences
 5-1 Higashiyama, Myodaiji, Okazaki, 444-8787 (Japan)
 and
 Graduate School of Pharmaceutical Sciences, Nagoya City University
 3-1 Tanabe-dori, Mizuho-ku, Nagoya, Aichi, 467-8603 (Japan)

 Supporting information and the ORCID identification number(s) for the author(s) of this article can be found under:
 <https://doi.org/10.1002/anie.202102774>

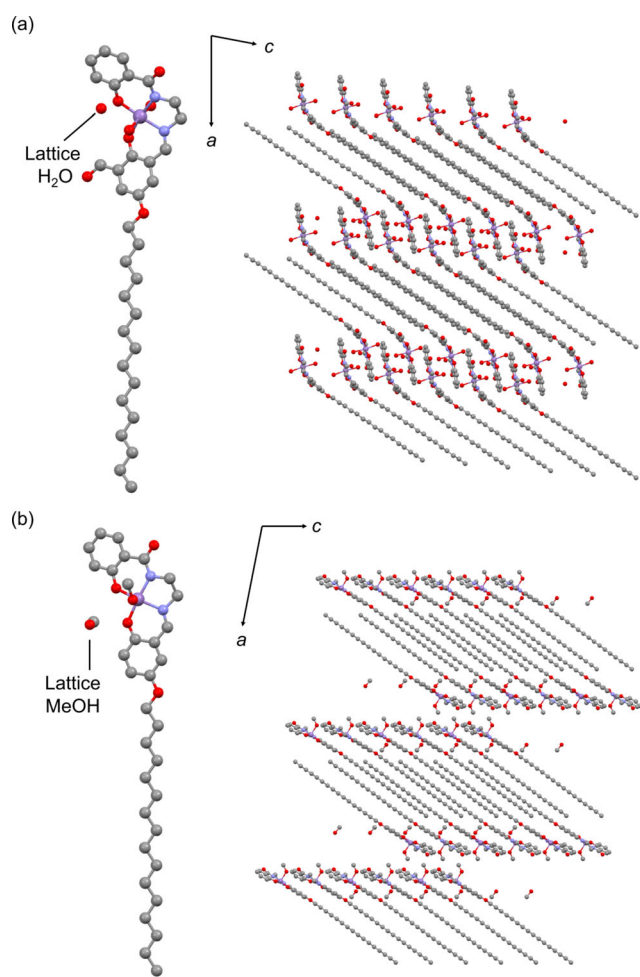


Figure 1. Crystal structures of a) **1**·**3H**₂**O** and b) **2**·**2MeOH**-color code: purple (Mn), gray (C), blue (N), and red (O). H atoms are omitted for clarity.^[17]

aldehyde substituents. The two lipids consist of amphiphilic molecules packed separately between hydrophilic and hydrophobic domains: manganese complex cores incorporating the respective N₂O₂ tetradentate ligands form hydrophilic domains, and alkyl chains with sixteen carbon atoms form hydrophobic (lipophilic) domains (Figure 1). Lattice and coordinating solvent molecules were present in the hydrophilic domains, which were confirmed by thermogravimetry and the elemental analyses of **1**·**3H**₂**O** and **2**·**2MeOH** (Figure S1 and Figure S2). Before preparing hybrid liposomes of DMPC combined with **1** and **2**, we treated the crystals at 100 °C to remove the lattice and coordinating solvents.

We prepared the hybrids of DMPC with **1** and **2**, during which we found that DMPC/**1** hybrids produce corresponding liposomes and DMPC/**2** does not disperse in water but precipitates as aggregations (Figure S3). Dynamic light scattering measurements of the DMPC/**1**(*x*) hybrids at molar ratios *x* = 0.063, 0.13, and 0.25 revealed that DMPC/**1**(*x*) are liposomes, whose sizes decrease with increasing *x*, which indicates that the critical packing parameter of **1** involves large head groups (Table S2).^[3d] To investigate the miscibility of **1** in DMPC bilayers, the phase transition behavior of the

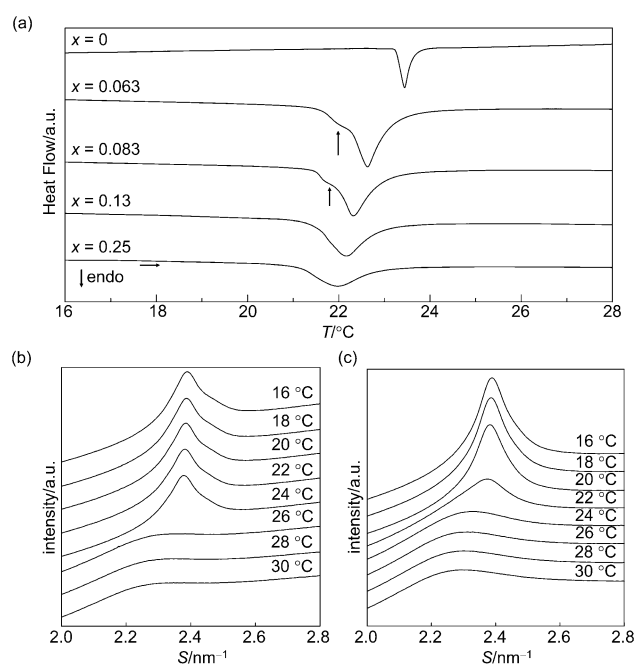


Figure 2. a) Differential scanning calorimetry results for 1,2-dimyristoyl-*sn*-glycero-3-phosphocholine (DMPC)/**1**(*x*) hybrids and variable temperature wide-angle X-ray scattering results for b) DMPC and c) DMPC/**1**(0.13).

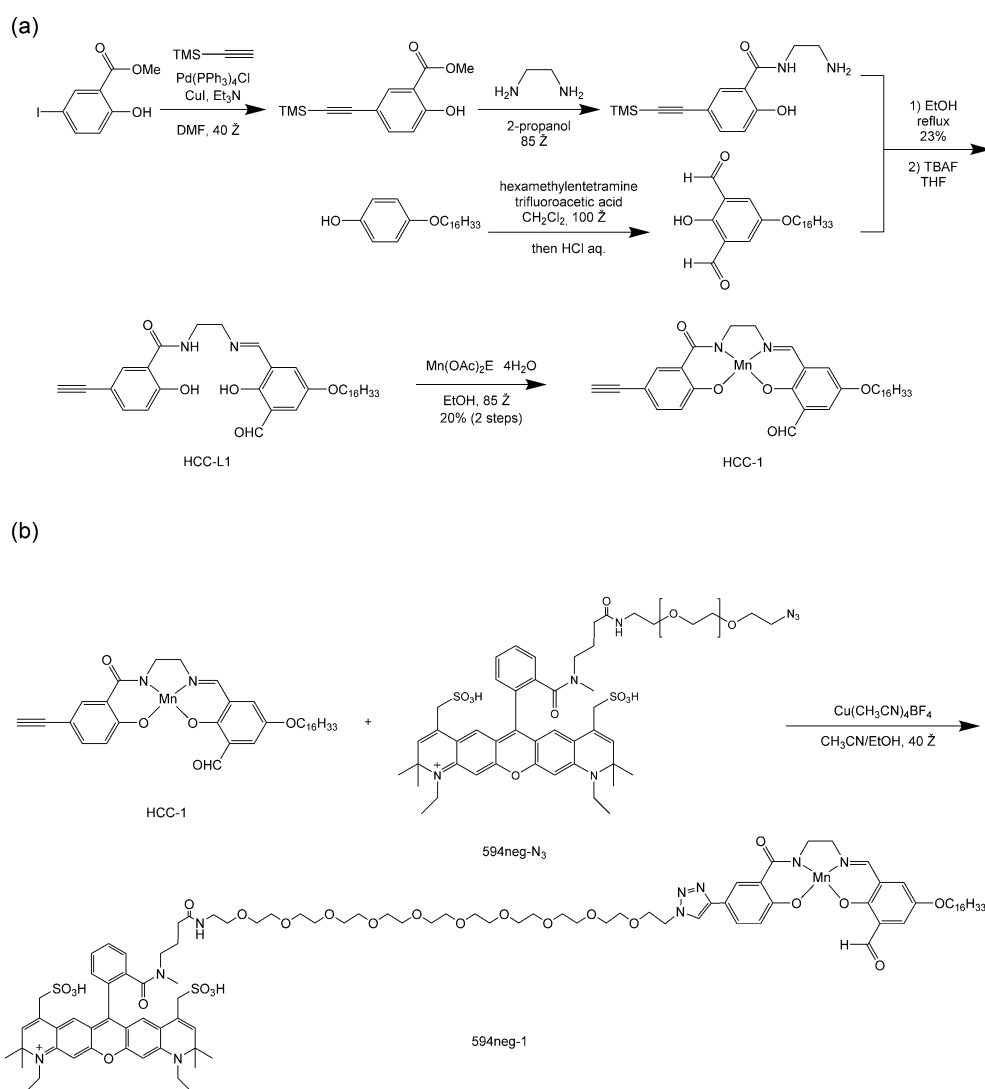
DMPC/**1**(*x*) hybrids (*x* = 0.063, 0.083, 0.13, and 0.25) were studied by differential scanning calorimetry (DSC) (Figure 2a). The lipid bilayers of DMPC exhibited a phase transition from the low-temperature gel phase to a high-temperature fluid phase at the *T*_c of 23.4 °C (*x* = 0 in Figure 2a). In the case of the hybrid liposomes of DMPC/**1** (0.063) and DMPC/**1** (0.083), two peaks were observed, which demonstrate that introducing small amount of **1** into the DMPC induced phase separations. DMPC/**1** (0.063) showed a large peak at 22.6 °C and a small shoulder with a peak top at 22.0 °C (Figure 2a). Similarly, DMPC/**1** (0.083) showed two peaks at 22.3 °C and 21.7 °C. In contrast, DMPC/**1** (0.13) and DMPC/**1** (0.25) showed a single and a broad peak at *T*_c = 22.0 °C and 21.9 °C, respectively. Total enthalpy of the phase transitions in DMPC/**1**(*x*) decreased gradually as the ratio of **1** increased (Table S3). The resultant decrease in transition temperature and enthalpy suggest that **1** is hybridized with DMPC, disturbing their lipid packings. These DSC results demonstrate that DMPC/**1** (0.063) and DMPC/**1** (0.083) consist of separated domains: one at a low *T*_c, which incorporates highly concentrated **1** (*H domain*), and the other at a high *T*_c, which incorporates less concentrated **1** (*L domain*). On the other hand, DMPC/**1** (0.13) and DMPC/**1** (0.25) were formed by the respective single *H domains*. We confirmed the *H domain* exhibited its phase transition between the gel and fluid phases with a lower *T*_c than DMPC by variable temperature wide-angle X-ray scattering (VT-WAXS) from 16 °C to 30 °C for multilamella vesicles of the pristine DMPC and DMPC/**1** (0.13) (Figure 2b,c and Figure S4). The broad diffraction peaks at higher temperatures above *T*_c indicate that fluid phases form, and their

disordered structures are attributed to the melting of carbon chains. It is noted that no tilted carbon chains were present in the gel phase of DMPC/**1** (0.13) as opposed to that of pristine DMPC.^[9] This structural difference would impact membrane thickness of DMPC/**1** (0.13). The small-angle X-ray scattering (SAXS) results for DMPC and DMPC/**1** (0.13) demonstrate slightly different peak positions at room temperature, indicating that DMPC/**1** (0.13) has thicker membranes than DMPC (Figure S5).

In multiple-lipid coassemblies, strong immiscibility between lipids gives separated regions such as gel-gel and gel-fluid phases at temperatures below the T_c .^[10] On the other hand, the separated domains with the phases usually disappear immediately above the T_c ; thus, both regions become miscible fluids with a single phase of blended lipids.^[10] Thus, to visually investigate the phase behavior in the DMPC/**1** (0.063), we carried out fluorescent microscopy for its giant-unilamellar vesicles (GUVs). As a fluorescent dye, a β -BODIPYTM FL C₁₂-HPC with green emission (bodipy-PC;

$\lambda_{ex} = 470$ nm) assembling in fluid areas was used.^[11] Furthermore, to identify the position of **1** in the GUVs, we synthesized a luminescent derivative metal complex lipid of **594neg-1** using a red emission probe (**594neg**; $\lambda_{ex} = 603$ nm) through a click reaction using **594neg-N₃** having an azide group^[12] and **HCC-1** having an ethynyl group at the terminal position of **1** (Scheme 1 and Figure S6). GUVs of DMPC/**1** (0.063) containing both bodipy-PC and **594neg-1** at 0.2% molar ratios were prepared by an electroformation method. Note that the respective bodipy-PC and **594neg-1**, and their coexistence were found to have no effect on domain formation in the GUVs without **1** (Figure S7).

The GUV images of DMPC/**1** (0.063) at 30 °C show green fluorescent regions and dark regions are separated (Figures 3 (left) and Figure S8). Moreover, areas showing red emissions of **594neg-1** correspond to the green fluorescent regions in the overlay image (Figure 3 (middle and right)). Thus, the separated green regions incorporating bodipy-PC are attributable to the *H domain* with a high concentration of **1**,



Scheme 1. Syntheses of a) **HCC-1** and b) **594neg-1**.

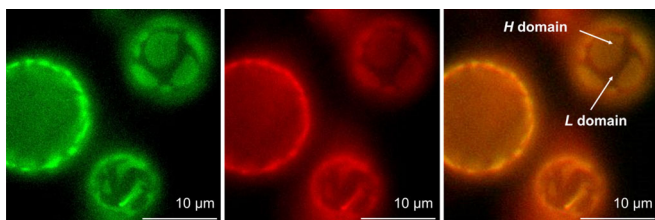


Figure 3. GUV images of DMPC/1(0.063) under excitation by 470 (left) and 560 nm (middle) and their overlay (right) at 30°C. GUVs at the upper right and lower corners show the corresponding surface images while one at the left shows the sliced image.

whereas, the dark regions with lower fluidity than occurring an accumulation of bodipy-PC are the *L domain* with a low concentration of **1**. Since 30°C is above the T_c of the *H* and *L domains*, the whole GUVs are in the fluid phase with disordered structures as demonstrated by VT-WAXS. Moreover, the fluid phase of both domains separated in the GUVs were proved by the dissolution phenomenon with a detergent, Triton X-100 (Figure S9).^[13] Therefore, we conclude that the observed phase separations in the GUVs are rarely visible “fluid–fluid” phase separations between the *H* and *L domains*.

Furthermore, variable temperature fluorescent microscopy measurements demonstrated that visible fluid–fluid phase separations remained in the temperature range between 30°C and 37°C (Figure 4a). With increase in temperature, the shape of the separated domains and GUVs changed, and mobility of the lipids increased. On the other hand, the phase separations were maintained up to 37°C. Around 37°C, the whole surface of the GUVs shows uniform emissions without phase separations (Figure 4a). These results reveal that both

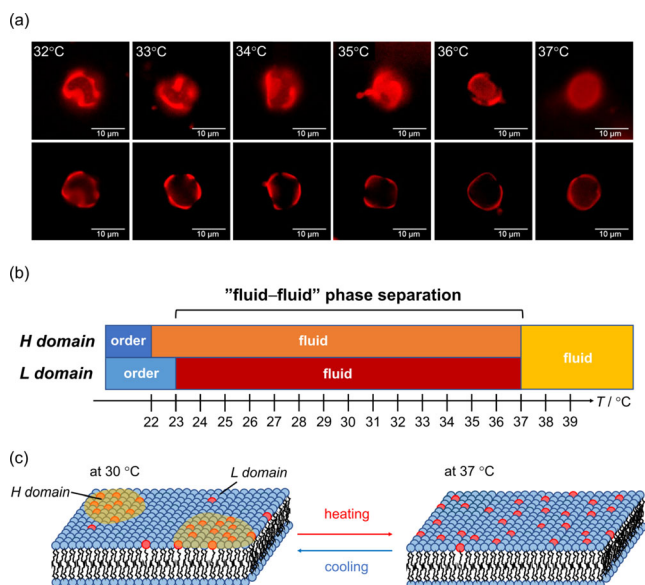


Figure 4. a) VT-fluorescent microscopy images of DMPC/1(0.063) during the heating process. The upper images display the surface of GUVs and the lower show the sliced images. b) Phase diagram of DMPC/1(0.063), and c) schematic representation of the phase separation. Blue and red amphiphiles indicate DMPC and **1**, respectively.

domains remained separated up to a temperature of at least 15°C above the T_c (Figure 4b). Moreover, we confirmed that the separated domains formed again by cooling, resulting in the reversible transition between the “fluid–fluid phase separation” and fluid uniform phases (Figure 4c and Figure S10).

Infrared (IR) spectroscopy revealed that the fluid–fluid phase separation phenomenon in DMPC/1(x) is attributed to the intermolecular interaction between DMPC and **1**. The pristine DMPC liposomes exhibited a stretching mode of the phosphate group ($\nu_{\text{O=P=O}}$) at 1232 cm^{-1} (Figure S11).^[14] This mode was observed at the same wavenumber in the aggregations of DMPC/2 (0.13), whereas DMPC/1 (0.13) displayed a peak of $\nu_{\text{O=P=O}}$ at 1228 cm^{-1} (Figure S11). Therefore, this shift involves the aldehyde group of **1** interacting with DMPC via its phosphate groups in the hydrophilic parts of membranes. Such intermolecular interaction leads to changing membrane properties such as stiffness and thickness. Lower T_c of the *H domain* than that of the *L domain* and the assembly nature of bodipy-PC on fluid regions^[11] indicate that the *H domain* is more fluid than the *L domain*. It was reported that the thickness mismatches between the separated domains notably stabilized the respective domains and impacted the domain sizes.^[6b] In this context, the difference in thickness between the *H* and *L domains* in the DMPC/1 hybrids indicated by SAXS results could account for the resultant phase separations.

To the best of our knowledge, only three cases of similar fluid–fluid phase separation in binary lipid bilayer membranes have been reported thus far: 1,2-dipalmitoyl-*sn*-glycero-3-phosphoethanolamine (DPPE) and 1,2-dierucoyl-*sn*-glycero-3-phosphocholine membranes,^[15a–c] dihydrosphingomyelin (DHSM) and 1,2-dioleoyl-*sn*-glycero-3-phosphocholine membranes,^[15d] and phosphatidylcholine and phosphatidylserine (PS) with Ca^{2+} ion systems.^[15e–g] In the former two cases, the hydrogen bonds between DPPE or DHSM lipids predominate to form the respective DPPE- and DHSM-rich domains separated from other lipid species. In the latter case, Ca^{2+} interacts with the head groups of PS lipids, allowing the formation of PS-rich domains as $\text{Ca}(\text{PS})_2$ against the PS-PS electrostatic repulsion, which tends to stabilize the mixed-lipids phase. These three cases provide “more rigid” regions formed by the aggregation of single lipid species than the other surrounding lipid regions. In contrast, **1** demonstrates the ability to produce separated “soft domains,” wherein it works as a “dopant” coassembled with the DMPC molecules, resulting in characteristic fluid–fluid phase separations. It is well-known that surfactants with a single hydrocarbon chain destabilize and break lipid packing structures.^[13,16] This is consistent with the effects of **2** on the DMPC membranes, yielding aggregations rather than bilayers (Figure S3, Figure S5 and Figure S12). A similar effect might exist in the hydrophobic part of **1** systems as indicated by the lower transition temperature and enthalpy of the *H domains* than those of the DMPC membranes. However, the intermolecular interaction of the metal complex cores with the aldehydes of **1** in the hydrophilic parts is key to preventing the break of membranes and keep up the characteristic fluid regions.

We synthesized metal complex lipid **1**, which produced separated domains with their respective fluid phases in DMPC membranes above the main transition temperature. This is the first demonstration of fluid–fluid phase separation of lipid membranes using a metal complex lipid. The phase separations were retained up to 37 °C, which is a very high temperature taking into account the main transition temperature of DMPC (23 °C). The fluorescent probe was attached with the metal complex cores via the click reaction. We speculate that **HCC-1** will also be applicable for constructing artificially separated platforms, assembling other functional molecules in lipid bilayers. This study provides new insights into the design of molecular probes for the chemical control of lipid distributions and assemblies in fluid membranes.

Acknowledgements

This work was supported by JSPS Grant-in-Aid for Young Scientists JP18K14245 and JSPS Grant-in-Aid for Scientific Research on Innovative Areas, Mixed Anion JP19H04701. This work was also supported by KAKENHI Grant-in-Aid for Scientific Research (A) JP17H01200. This work was partially supported by the Cooperative Research Program of “Network Joint Research Centre for Materials and Devices”, and Kyushu Synchrotron Light Research Center (SAGA-LS) 1807056F. This research was supported by Joint Research by Institute for Molecular Science (IMS) (IMS program No.101, 102, and 20–101). We thank Prof. Hayato Ishikawa and Mr. Kenta Rakumitsu (Kumamoto university) for the synthesis of **HCC-L1** and writing of the organic synthesis section.

Conflict of interest

The authors declare no conflict of interest.

Keywords: amphiphile · lipid bilayer · metal-complex lipid · phase separation · supramolecules

- [1] a) T. Aida, E. W. Meijer, S. I. Stupp, *Science* **2012**, *335*, 813–817; b) R. Kaur, S. K. Mehta, *Coord. Chem. Rev.* **2014**, *262*, 37–54; c) T. Homma, K. Harano, H. Isobe, E. Nakamura, *J. Am. Chem. Soc.* **2011**, *133*, 6364–6370; d) S. G. Zhang, *Nat. Biotechnol.* **2003**, *21*, 1171–1178; e) S. P. Wang, W. Lin, X. L. Wang, T. Y. Cen, H. J. Xie, J. Y. Huang, B. Y. Zhu, Z. B. Zhang, A. X. Song, J. C. Hao, J. Wu, S. J. Li, *Nat. Commun.* **2019**, *10*, 1399; f) M. Dubois, B. Deme, T. Gulik-Krzywicki, J. C. Dedieu, C. Vautrin, S. Desert, E. Perez, T. Zemb, *Nature* **2001**, *411*, 672–675; g) M. A. Greenfield, L. C. Palmer, G. Vernizzi, M. O. de la Cruz, S. I. Stupp, *J. Am. Chem. Soc.* **2009**, *131*, 12030–12031.
- [2] a) K. Simons, E. Ikonen, *Nature* **1997**, *387*, 569–572; b) W. M. Aumiller, C. D. Keating, *Nat. Chem.* **2016**, *8*, 129–137; c) A. K. Rha, D. Das, O. Taran, Y. G. Ke, A. K. Mehta, D. G. Lynn, *Angew. Chem. Int. Ed.* **2020**, *59*, 358–363; *Angew. Chem.* **2020**, *132*, 366–371.
- [3] a) H. A. M. Ardoña, E. R. Draper, F. Citossi, M. Wallace, L. C. Serpell, D. J. Adams, J. D. Tovar, *J. Am. Chem. Soc.* **2017**, *139*, 8685–8692; b) A. López-Andarías, C. Atienza, J. López-Andarías, W. Matsuda, T. Sakurai, S. Seki, N. Martín, *J. Mater. Chem. C* **2019**, *7*, 6649–6655; c) L. K. Ji, Y. T. Sang, G. H. Ouyang, D. Yang, P. F. Duan, Y. Q. Jiang, M. H. Liu, *Angew. Chem. Int. Ed.* **2019**, *58*, 844–848; *Angew. Chem.* **2019**, *131*, 854–858; d) R. Ohtani, T. Tokita, T. Takaya, K. Iwata, M. Kinoshita, N. Matsumori, M. Nakamura, L. F. Lindoy, S. Hayami, *Chem. Commun.* **2017**, 53, 13249–13252; e) C. Yuan, M. Yang, X. Ren, Q. Zou, X. Yan, *Angew. Chem. Int. Ed.* **2020**, *59*, 17456–17460; *Angew. Chem.* **2020**, *132*, 17609–17613.
- [4] a) A. Ianiro, H. L. Wu, M. M. J. van Rijt, M. P. Vena, A. D. A. Keizer, A. C. C. Esteves, R. Tuinier, H. Friedrich, N. Sommerdijk, J. P. Patterson, *Nat. Chem.* **2019**, *11*, 320–328; b) J. R. Viereg, M. Lueckheide, A. B. Marciel, L. Leon, A. J. Bologna, J. R. Rivera, M. V. Tirrell, *J. Am. Chem. Soc.* **2018**, *140*, 1632–1638; c) S. Alberti, A. Gladfelter, T. Mittag, *Cell* **2019**, *176*, 419–434; d) G. A. Ilevbare, L. S. Taylor, *Cryst. Growth Des.* **2013**, *13*, 1497–1509; e) S. S. Kim, D. R. Lloyd, *Polymer* **1992**, *33*, 1047–1057; f) H. Le Ferrand, M. Duchamp, B. Gabryelczyk, H. Cai, A. Miserez, *J. Am. Chem. Soc.* **2019**, *141*, 7202–7210.
- [5] a) D. A. Brown, E. London, *J. Biol. Chem.* **2000**, *275*, 17221–17224; b) G. T. Noble, F. L. Craven, J. Voglmeir, R. Sardzik, S. L. Flitsch, S. J. Webb, *J. Am. Chem. Soc.* **2012**, *134*, 13010–13017; c) R. J. Mart, K. P. Liem, X. Wang, S. J. Webb, *J. Am. Chem. Soc.* **2006**, *128*, 14462–14463; d) S. Sonnino, A. Prinetti, L. Mauri, V. Chigorno, G. Tettamanti, *Chem. Rev.* **2006**, *106*, 2111–2125.
- [6] a) R. Ziblat, L. Leiserowitz, L. Addadi, *Angew. Chem. Int. Ed.* **2011**, *50*, 3620–3629; *Angew. Chem.* **2011**, *123*, 3700–3710; b) F. A. Heberle, R. S. Petruzielo, J. Pan, P. Drazba, N. Kucerka, R. F. Standaert, G. W. Feigenson, J. Katsaras, *J. Am. Chem. Soc.* **2013**, *135*, 6853–6859.
- [7] a) R. Sakla, D. A. Jose, *ACS Appl. Mater. Interfaces* **2018**, *10*, 14214–14220; b) Y. G. Li, L. Chen, Y. Y. Ai, E. Y. H. Hong, A. K. W. Chan, V. W. W. Yam, *J. Am. Chem. Soc.* **2017**, *139*, 13858–13866; c) X. Roy, L. K. Thompson, N. Coombs, M. J. MacLachlan, *Angew. Chem. Int. Ed.* **2008**, *47*, 511–514; *Angew. Chem.* **2008**, *120*, 521–524; d) J. Liu, M. A. Morikawa, N. Kimizuka, *J. Am. Chem. Soc.* **2011**, *133*, 17370–17374; e) B. Gruber, E. Kataev, J. Aschenbrenner, S. Stadlbauer, B. Koenig, *J. Am. Chem. Soc.* **2011**, *133*, 20704–20707.
- [8] R. Ohtani, K. Kawano, M. Kinoshita, S. Yanaka, H. Watanabe, K. Hirai, S. Futaki, N. Matsumori, H. Uji-i, M. Ohba, K. Kato, S. Hayami, *Angew. Chem. Int. Ed.* **2020**, *59*, 17931–17937; *Angew. Chem.* **2020**, *132*, 18087–18093.
- [9] S. Tristram-Nagle, Y. F. Liu, J. Legleiter, J. F. Nagle, *Biophys. J.* **2002**, *83*, 3324–3335.
- [10] F. G. Wu, R. G. Wu, H. Y. Sun, Y. Z. Zheng, Z. W. Yu, *Phys. Chem. Chem. Phys.* **2014**, *16*, 15307–15318.
- [11] A. S. Klymchenko, R. Kreder, *Chem. Biol.* **2014**, *21*, 97–113.
- [12] M. Kinoshita, K. G. N. Suzuki, N. Matsumori, M. Takada, H. Ano, K. Morigaki, M. Abe, A. Makino, T. Kobayashi, K. M. Hirose, T. K. Fujiwara, A. Kusumi, M. Murata, *J. Cell Biol.* **2017**, *216*, 1183–1204.
- [13] a) J. Sot, L. A. Bagatolli, F. M. Goni, A. Alonso, *Biophys. J.* **2006**, *90*, 903–914; b) A. A. Ribeiro, E. A. Dennis, *Biochim. Biophys. Acta Biomembr.* **1974**, *332*, 26–35.
- [14] W. Pohle, C. Selle, D. R. Gauger, R. Zantl, F. Artzner, J. O. Radler, *Phys. Chem. Chem. Phys.* **2000**, *2*, 4642–4650.
- [15] a) S. H. W. Wu, H. M. McConnell, *Biochemistry* **1975**, *14*, 847–854; b) J. M. Seddon, K. Harlos, D. Marsh, *J. Biol. Chem.* **1983**, *258*, 3850–3854; c) H. Chang, R. M. Epand, *Biochim. Biophys. Acta Biomembr.* **1983**, *728*, 319–324; d) M. Kinoshita, N. Matsumori, M. Murata, *Biochim. Biophys. Acta Biomembr.* **2014**, *1838*, 1372–1381; e) A. K. Hinderliter, J. Y. Huang, G. W. Feigenson, *Biophys. J.* **1994**, *67*, 1906–1911; f) J. Y. Huang, G. W. Feigenson, *Biophys. J.* **1993**, *65*, 1788–1794; g) J. Y. Huang, J. E. Swanson, A. R. G. Dibble, A. K. Hinderliter, G. W. Feigenson, *Biophys. J.* **1993**, *64*, 413–425.

- [16] a) H. Heerklotz, *Biophys. J.* **2002**, *83*, 2693–2701; b) H. Heerklotz, H. Szadkowska, T. Anderson, J. Seelig, *J. Mol. Biol.* **2003**, *329*, 793–799.
- [17] Deposition Numbers 2033868 and 2033869 (for **1·3H₂O** and **2·2MeOH**) contain the supplementary crystallographic data for this paper. These data are provided free of charge by the joint Cambridge Crystallographic Data Centre and Fachinforma-

tionszentrum Karlsruhe Access Structures service www.ccdc.cam.ac.uk/structures.

Manuscript received: February 24, 2021
Accepted manuscript online: March 15, 2021
Version of record online: ■ ■ ■ ■, ■ ■ ■ ■

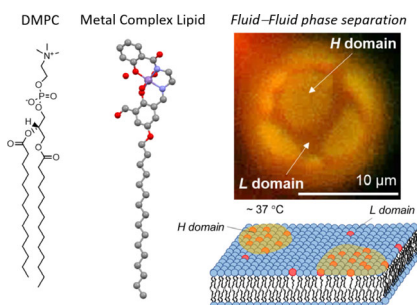
Communications



Supramolecular Chemistry

R. Ohtani,* Y. Anegawa, H. Watanabe,
Y. Tajima, M. Kinoshita,* N. Matsumori,
K. Kawano, S. Yanaka, K. Kato,
M. Nakamura, M. Ohba,
S. Hayami* ————— ■■■■-■■■■

Metal Complex Lipids for Fluid–Fluid
Phase Separation in Coassembled
Phospholipid Membranes



Coassembly of metal complex lipids with DMPC demonstrates a very rare fluid–fluid phase separation up to 37°C.